Exciton dynamics in GaAs quantum wells under resonant excitation

A. Vinattieri,* Jagdeep Shah, T. C. Damen, and D. S. Kim
AT&T Bell Laboratories, Holmdel, New Jersey 07733

L. N. Pfeiffer
AT&T Bell Laboratories, Murray Hill, New Jersey 07974

M. Z. Maialle and L. J. Sham
University of California at San Diego, La Jolla, California 92093
(Received 10 May 1994)

We present a comprehensive investigation of the dynamics of resonantly excited nonthermal excitons in high-quality GaAs/$Al_xGa_{1-x}As$ multiple-quantum-well structures on picosecond time scales. The dynamics was investigated using the luminescence upconversion technique with two independently tunable, synchronized dye lasers, which allowed measurements of the time evolution of polarized resonant luminescence with 4-ps time resolution. We show that the evolution of excitons from the initial nonthermal distribution to the thermal regime is determined by three different physical processes: (1) the enhanced radiative recombination of the metastable two-dimensional exciton polaritons, (2) the spin relaxation of excitons, and (3) the momentum relaxation of excitons. We also show that these three processes have comparable rates, so that a unified model accounting for all important processes is essential for a correct analysis of the experimental results. Using such a unified model, we have determined the rates of these processes contributing to the initial relaxation of excitons as a function of quantum-well width, temperature, and applied electric field. Quantum confinement strongly influences the radiative recombination and spin relaxation of excitons, and our study provides significant insights into these processes in quantum wells. The measured radiative recombination rate is about a factor of 2 smaller than calculated theoretically. The electric field reduces the electron-hole overlap and hence reduces the spin-relaxation rate of excitons between the optically allowed $|\pm 1\rangle$ states. The measured variation is in good qualitative agreement with a recent theory, but somewhat slower than predicted by the theory.

I. INTRODUCTION

Excitons play a major role in the optical properties of quantum wells (QW's) near the fundamental absorption edge because the binding energies and the oscillator strengths of excitons in QW's are significantly enhanced compared to the corresponding bulk semiconductors. Excitonic effects in quantum wells have been investigated extensively during the past decade.[1] Of the many interesting properties of excitons, the dynamics of excitons is of particular interest because of its fundamental importance, and also because it determines the speed of devices based on excitons in QW's. The dynamical processes of excitons have been extensively investigated from both theoretical and experimental points of view. There are many reports in the literature on the nonlinear dynamics of excitons,[2] such as the ac Stark effect, bleaching of excitons by phase-space filling, and screening, broadening of excitonic resonance. We will not be concerned with these nonlinear aspects of exciton dynamics in this paper. Rather we will be interested in the radiative recombination of excitons, and in the exciton relaxation processes such as the formation dynamics of excitons, scattering of excitons by other excitons and free carriers, interaction of excitons with phonons, interfaces and defects, and spin relaxation of excitons.

Resonant and nonresonant excitations of excitons provide access to completely different aspects of exciton dynamics. Most of the experimental work has been performed using *nonresonant excitation* in which the continuum states are initially excited. The following picture has emerged as a result of earlier studies.[3] The photoexcited electron-hole pairs thermalize, and the pairs with low kinetic energies emit acoustic phonons to form excitons at large in-plane wave vectors $K_{\parallel}$ in <20 ps. These large wave-vector excitons interact among themselves and with phonons, and relax to $K_{\parallel}=0$ excitons which can radiate. The initial dynamics of nonresonantly excited luminescence in intrinsic samples is dominated by this relaxation process and shows a slow rise of several hundred picoseconds.[3-6] In samples exhibiting localization effects, relaxation through localized states plays a major role and also modifies the radiative recombination kinetics.[7] However, in this paper, we will be exclusively concerned with high-quality, intrinsic samples in which such localization effects are not important. During the process of formation of excitons and relaxation to $K_{\parallel}=0$, excitons also undergo spin relaxation which has been investigated in intrinsic[8,9] as well as modulation-doped quantum wells using polarized time-resolved luminescence spectroscopy.[10]

The recombination dynamics of nonresonantly excited excitons in GaAs QW's has also been investigated quite extensively as a function of well-width and lattice temper-

ature[11] and found to be controlled by the thermalized exciton distribution. The main result of these studies is that the luminescence decay time in high-quality samples is typically several hundred picoseconds [about an order of magnitude shorter than those in bulk GaAs (Ref. 12)], and the decay time decreases with decreasing well width and also with decreasing temperature. The latter behavior was explained on the basis of decreased coherence volume and decreased fraction of excitons within the homogeneous linewidth with increasing temperatures.[11] We note that the exponential decay of luminescence is characteristic of a thermalized exciton distribution and provides no information about the nonthermal dynamics of excitons.

The dynamics of *resonantly-excited excitons* is, in some sense, the exact opposite of the nonresonant case, and is determined by the relaxation of the cold, nonthermal photoexcited excitons to thermalized excitons. Therefore, the time evolution of luminescence provides direct information about the nonthermal dynamics of excitons which is governed by several processes. The dynamics of resonantly-excited excitons is only beginning to be investigated. Recent experiments in GaAs QW's include investigation of scattering to different in-plane momentum states,[8] exciton ionization,[13] spin relaxation of excitons, electrons and holes,[8,14] and the recombination dynamics of excitons.[15–17] Most of these studies have focused on only one or two aspects of exciton dynamics and did not develop a comprehensive picture of exciton dynamics following resonant excitation. Two issues need particular attention, and form the focus of our work: (1) *Recombination dynamics* of resonantly excited excitons is of special interest because, unlike the stationary three-dimensional (3D) exciton polariton,[18] the 2D exciton polariton is metastable with a finite radiative lifetime.[19,20] This introduces *qualitatively different features* for the 2D excitons and strongly influences the dynamics following resonant excitation. (2) Qualitatively different features are also introduced in the *spin-relaxation dynamics* by quantum confinement. The electron-hole exchange interaction responsible for the spin flip of excitons between optically allowed states is enhanced by confinement[21] and needs to be studied quantitatively. The hole spin flip is also different from the bulk because of the lifting of the degeneracy in the valence bands at the center of the Brillouin zone.[22]

In this paper, we present extensive experimental results on the dynamics of resonantly-excited excitons for GaAs QW's of different well widths at different temperatures, excitation intensities and applied electric fields. The results are obtained by a recently developed luminescence upconversion technique which uses two synchronized picosecond lasers at different wavelengths to permit time-resolved resonant luminescence measurements with a time resolution of 3–4 ps. Since our recent results have shown[23] that many of the physical processes determining the dynamics of resonantly-excited excitons occur on the same time scale, we have analyzed our results on the basis of *a unified model* which takes into account all the dynamical processes of excitons rather than just one or two as in previous investigations. This allows us to obtain *quantitative information* on the exciton momentum and spin-relaxation rates as well as on the exciton radiative recombination rates, and to develop a comprehensive picture of exciton dynamics following resonant excitation. In particular, our results elucidate the role of the enhanced recombination of 2D excitons and the role of exciton spin relaxation in the dynamics of excitons in quantum wells.

The plan for the paper is as follows. In Sec. II we discuss some basic concepts relevant to exciton relaxation and recombination dynamics. In Sec. III, we discuss the resonant luminescence upconversion technique that has allowed us to investigate the dynamics of resonantly-excited excitons with better time resolution than before. In Sec. IV, we present representative experimental results and in Sec. V we present a unified model containing all essential aspects of exciton relaxation and recombination dynamics. In Sec. VI we apply this model to analyze our experimental data and obtain quantitative information about various relaxation and recombination rates. A summary and conclusions are presented in Sec. VII.

II. BASIC CONCEPTS

In this section, we briefly discuss some of the basic concepts relevant to the dynamics of resonantly-excited excitons in QW's. The discussion can be naturally divided into three parts: (A) Excitation, (B) relaxation and thermalization, and (C) recombination.

A. Resonant excitation of excitons

Resonant excitation with an excitation beam propagating at an angle α with respect to the growth direction z of the QW produces excitons with an in-plane component of the momentum $K_{\parallel}$ given by

$$K_{\parallel}=K_0 \sin\alpha \ , \tag{1}$$

where K_0 is the photon momentum, approximately a few times 10^5 cm^{-1}, so that E_0, the kinetic energy of the exciton at $K_{\parallel}=K_0$ is ~ 0.1 meV. A continuous-wave (cw) excitation creates excitons within the homogeneous linewidth Γ_h of E_0, where Γ_h is typically several times E_0.[24] The initial distribution is nonthermal, and the average energy is less than $k_B T$ for T greater than few degrees Kelvin. Excitation with a short pulse creates coherent polarization and virtual population within the spectral width of the exciting laser. During this coherent regime, it is possible to observe resonant Rayleigh scattering (RRS) from these excitons[25,26] using techniques similar to those used in our investigation. However, as we will discuss later, our results do not show any contribution from RRS. We will therefore not consider the coherent regime in this paper, although it is a subject of intense current research.[27] In the case investigated here, the excitation pulse produces a δ-like anisotropic distribution of excitons in the momentum space. If the excitation is with circularly polarized light, then the initial population is only in the $|+1\rangle$ or the $|-1\rangle$ exciton state. The measured temporal dynamics of resonantly-excited luminescence is determined by the relaxation, thermaliza-

tion, and recombination dynamics of this initial nonthermal distribution.

B. Relaxation and thermalization

We discuss in this section several physical processes that determine the relaxation and thermalization of resonantly-excited excitons.

1. Elastic and quasielastic dephasing processes

Radiative recombination from the initial anisotropic exciton distribution created by photoexcitation occurs only in the reflection and transmission direction for a perfect quantum well. Scattering from impurities, interface roughness, or interaction with very-low-energy acoustic phonons redistributes the excitons in the momentum space, and within the homogeneous linewidth Γ_h related to the characteristic dephasing time T_2 by $T_2=2\hbar/\Gamma_h$. In high-quality samples T_2 is typically a few picoseconds, corresponding to Γ_h of a few tenths of meV.[24] The initial anisotropic radiation pattern becomes more isotropic as this redistribution takes place. We are not aware of any experimental investigation of the changing radiation pattern.

2. Momentum scattering

Excitons can interact with acoustic and optical phonons through various mechanisms. For resonantly created excitons, only absorption of phonons is important so that at low temperatures, only acoustic phonon scattering through piezoelectric and deformation potential interactions need be considered. These have been investigated quite extensively from a theoretical point of view.[28,29] The scattering rate for $K_{\parallel}=0$ excitons by deformation potential scattering is given by

$$W_{K_0} \propto \frac{TM}{\rho u^2 L}(D_c-D_v)^2 , \tag{2}$$

where T is the temperature, M is the exciton mass, ρ is the density of GaAs, u the sound velocity, D_c and D_v the deformation potential for the conduction and valence band, and L is the well thickness. W_{K_0} depends inversely on the well thickness, the interaction being less effective in wider wells. Scattering rates are of the order of 1×10^{11} s^{-1} for a 150-Å QW at a lattice temperature of 10 K.[28]

3. Exciton spin relaxation

The basic mechanisms for spin relaxation in bulk semiconductors are strongly affected by the confinement introduced by the quantum wells. In particular, we can emphasize three different aspects that modify the spin relaxation in QW's with respect to bulk: (a) the lifting of the degeneracy in the valence band between the heavy-hole (HH) and the light-hole (LH) subbands removes the mixing at $K_{\parallel}=0$ and moves it to larger $K_{\parallel}$, (b) the confinement in the z direction increases the overlap between the electron and hole wave functions and makes the electron-hole exchange interaction more important, and (c) the higher carrier mobility in 2D system affects the spin relaxation, for example, by the Dyakonov-Perel mechanisms.[30]

Spin relaxation equilibrates the populations of excitons within its four spin states $|\pm1\rangle$ and $|\pm2\rangle$. A comprehensive theory of the exciton spin dynamics has been published recently.[21] The exciton spin relaxation between the optically-allowed states can occur in a direct, single-step process driven by the electron-hole exchange interaction, which consists of a long-range and a short-range term. It was shown that the long-range contribution, which originates from the exciton dipole-dipole interaction and depends on $K_{\parallel}$, dominates the short-range interaction which requires the mixing of the valence bands.

In addition, the electron or the hole within an exciton can flip its spin and lead to a transition between an optically-allowed and forbidden state (e.g., from $|+1\rangle$ to $|+2\rangle$). Two such transitions, one involving an electron and the other involving a hole, are necessary to go between optically-allowed exciton states. The exchange interaction responsible for the direct process depends on the electron-hole overlap integral[31] which can be controlled by either varying the well width or by applying an electric field along the z direction. The second mechanism, i.e., the independent spin flip of each carrier inside the exciton, is not affected by a change in the wave function overlap. The hole spin relaxation is modified by the different band mixing (compared to bulk) and spin relaxation of both carriers is influenced by the momentum relaxation which may be different in bulk and quantum wells. Time-resolved polarized luminescence spectroscopy provides a means of probing the spin dynamics of excitons.

C. Recombination of excitons in QW's

In a perfect, infinite bulk crystal the polariton (coupled photon-exciton mode) is a stationary mode with an infinite lifetime in the absence of scattering.[18] In order to conserve the crystal momentum, an exciton with a given momentum can interact only with one photon with the same momentum, neglecting Umklapp processes. Therefore, there is no density of the states for the radiative decay, but only a linear coupling between two discrete states, giving rise to stationary states, known as polaritons. Recombination can only occur at defects and boundaries and in the latter case the radiative rate corresponds to the probability of escaping from the crystal, thus dependent on the crystal size.[32] Experimentally, long photoluminescence (PL) decay times of the order of few nanoseconds have been measured in bulk GaAs.[12]

The breaking of the translational invariance along the z (growth) direction strongly modifies the nature of the polariton in 2D systems such as quantum wells,[33,19,20] and introduces qualitatively different features in the radiative recombination of excitons in QW. In fact, the momentum conservation is required only along the planes. Therefore an exciton with a given $K_{\parallel}$ can interact with photons with the same $K_{\parallel}$ but all possible values of K_z where K_z is the momentum component along the growth direction, providing a density of states for the decay.

It was shown that polaritons in QW's can be classified as either resonant polaritons with $K_{\parallel}\leq K_0$ or surface polaritons with $K_{\parallel}>K_0$.[20] The surface polariton is, in some

sense, the analog of the bulk polariton, and has an infinite lifetime. The resonant polariton can couple to photons and has a finite lifetime of the order of a few tens of picoseconds, depending on the well width.[34] Despite these theoretical predictions all the nonresonant experiments have reported long decay times for the excitonic PL as we discussed in the Introduction. This is because only a small fraction of excitons occupy the radiative states of the polariton at any time following nonresonant excitation in the continuum. The situation is completely different for resonantly-excited excitons because all the excitons are initially created in the radiative state. Therefore, the enhanced radiative recombination rate of the 2D exciton polariton can be expected to play a significant role in the dynamics of resonantly-excited excitons and this is one of the major points of interest in our investigation.

III. EXPERIMENTAL TECHNIQUES

Two dye lasers, synchronously pumped by the second harmonic of a mode-locked Nd:YLF laser, were used in the time-resolved experiments. A Styryl 9 dye laser, with 3 ps pulse width and 3-meV-spectral width, was used for resonantly exciting the sample at the heavy-hole excitons. A Rhodamine 6G dye laser with the same spectral and temporal characteristics was used for upconverting the collected luminescence in a 2-mm-long $LiIO_3$ crystal.[35] The use of two dye lasers at different frequencies allowed us to perform the resonant experiment with the upconversion technique, without being limited by the second harmonic of the pump laser. The time resolution of this setup (<5 ps) is limited by the jitter between the two lasers. The experimental conditions were such that only the HH excitonic band was excited and detected.

We investigated three high-quality $GaAs/Al_{0.3}Ga_{0.7}As$ samples with well width 80, 130, and 150 Å, respectively. The samples consist of 15 periods of GaAs wells embedded between $Al_{0.3}Ga_{0.7}As$ 150-Å barriers. On the 150-Å sample a transparent Schottky contact (Cr) was used to apply a reverse bias. The electric field in the sample was determined from measurements of the quantum confined Stark effect. cw PL and photoluminescence-excitation (PLE) spectra were measured for the sample characterization; no significant Stokes shift is observed between PL and PLE. The linewidth is 1 (3) meV for the 150-Å (80-Å) sample. The PL quantum efficiency remains constant in the explored temperature range (10–40 K). We conclude from this observation and the temperature-dependent decay rate data to be presented later that nonradiative processes are unimportant. The homogeneous broadening of excitons was determined using the standard two-beam four-wave-mixing experiments with 100 fs and 3 ps lasers tuned close to the HH exciton energy.

Luminescence experiments were performed with the samples mounted on the cold finger of a liquid He cryostat and with typical excitation density of 5×10^9 cm^{-2}. A nearly backscattering geometry was used: the beam was incident at an external angle of $\approx10°$ and the collection angle was $\approx20°$ to the normal, in the direction away from the reflected beam. In this configuration excitons with $K_{\parallel}\sim0$ are photoexcited. Left (right) circularly polarized light was used to resonantly excite the $|+1\rangle$ ($|-1\rangle$) excitons, and only the left circularly polarized emission was detected. We indicate with I^+ and I^- the PL intensity from the $|+1\rangle$ excitons when the optical pulse excites the $|+1\rangle$ and $|-1\rangle$ excitons, respectively. Measurements were also performed using linearly polarized excitation laser and detecting only the vertically polarized component of the PL. These results were consistent with the results and the analysis for circularly polarized data discussed here, and will not be discussed further in this paper. We indicate with S and D the total PL (sum) and the difference (D) between the two polarized components. Because the laser linewidth, used for exciting each sample, was always greater than the PL inhomogeneous linewidth, all of the HH band was excited; besides, due to the finite spectral resolution of the upconversion technique, no change was found spanning the detection energy within the HH band.

IV. REPRESENTATIVE EXPERIMENTAL RESULTS

Figure 1 shows the PL time evolution of I^+ and I^- for the 150-Å quantum well at 12 K. After an initial fast rise I^+ shows more than an order-of-magnitude decrease in the first 100 ps. I^- increases slowly and the two PL components almost equilibrate after ~100 ps. Figure 1(b) shows the total luminescence S and the difference D, along with the cross correlation of the two dye-laser pulses which indicates the time resolution of our experiments. Figure 1(c) shows the long-time behavior of the total luminescene S. The exponential decay at long times has a slope similar to that observed in nonresonant experiments,[11] indicating that the long-time dynamics is controlled by similar physical processes in the two cases. All three samples show qualitatively similar behavior.

We note that the initial decay of the luminescence [Figs. 1(a) and 1(b)] is much slower than the cross-correlation signal. We conclude from this that scattering

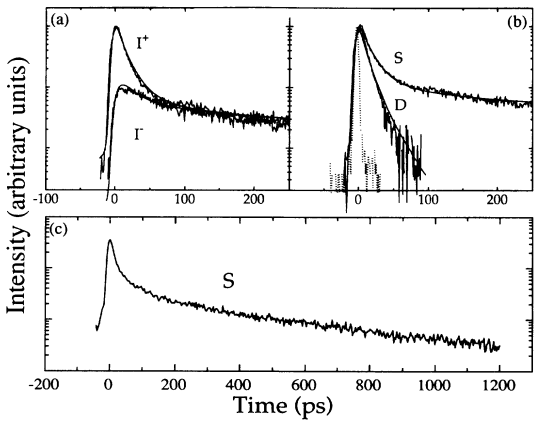

FIG. 1. PL decay for the 150-Å QW at 12 K at low excitation intensity. (a) Time evolution of I^+ and I^-. (b) Time evolution of the sum S and difference D. The dotted line is the cross-correlation signal, showing the experimental time resolution. (c) Long-time behavior of the sum S. In (a) and (b) the best fit to the experimental data, as discussed in the text, are also shown.

from surface roughness, which represented the major limitation in previous experimental reports, is not important in our experiment. Also, the initial decay of D has a time constant of 12 ps, a factor of four larger than $T_2/2$ determined from our four-wave mixing (FWM) experiments. Therefore the measured time evolution in the first 100 ps contains *important physical information about incoherent nonequilibrium exciton dynamics.*

In order to obtain a quantitative understanding of these results, we need to model the dynamics of resonantly excited excitons. Our earlier results[23] have shown that a unified model is essential for the correct interpretation of the data. We develop such a unified model in the next section.

V. A UNIFIED MODEL

Energy and momentum conservation requires that excitons with a given $K_{\parallel}$ vector can only radiate in a given direction, with a rate that depends on $K_{\parallel}$.[20,36] We simplify the picture and assume that the radiative recombination rate of excitons within the homogeneous Γ_h of E_0 is independent of $K_{\parallel}$, inversely proportional to Γ_h, and given by[36]

$$W_R=\frac{4E_0}{3\Gamma_h}(2\Gamma_0)\ , \tag{3}$$

where $2\Gamma_0$ is the fundamental radiative recombination rate of the exciton *population* at $K_{\parallel}=0$. With this simplification, the calculation of the time evolution of resonantly-excited luminescence is reduced to the calculation of the population of excitons in the radiative state corresponding to the polarization of the measured luminescence. The PL intensity at time t is given by

$$I(t)=W_R f(t)N(t)\ , \tag{4}$$

where $N(t)$ is the total population of excitons at time t, and $f(t)$ is the fraction of $N(t)$ in the spin state corresponding to the measured polarized luminescence. Note that f is a function of time for nonthermal distributions, and becomes independent of time only when the excitons reach thermal equilibrium with the lattice. The PL decay will be exponential at such times, with a decay rate W_D given by

$$W_D=W_R f_0=W_R\frac{\left[1-\exp\left[-\frac{\Gamma_h}{k_BT}\right]\right]}{\left[1+\exp\left[\frac{\Delta}{k_BT}\right]\right]}\ , \tag{5}$$

where f_0 is the value of $f(t)$ under thermal equilibrium and Δ is the exchange splitting between the $|\pm1\rangle$ and $|\pm2\rangle$ spin states.

We calculate the population of excitons in various spin and momentum states using the following simplified model (Fig. 2) which retains the essential features of the exciton dynamics as discussed in Sec. II. We consider the case when the incident photons generate excitons in the $|+1\rangle$ radiative state. Exciton spin-relaxation (with rate W_X) populates $|-1\rangle$ state, and electron or hole spin flip within the exciton (rates W_e and W_h, respectively) populates the dipole-inactive $|\pm2\rangle$ nonradiative (dark) states. We divide the manifold of $K_{\parallel}$ states into two sets, one for small $K_{\parallel}$ and the other for large $K_{\parallel}$. Each set contains four exciton states ($|\pm1\rangle$ and $|\pm2\rangle$). Acoustic-phonon absorption and emission induce transitions between these sets; we allow only spin-conserving transitions between the two sets with an effective scattering rate W_k. Each transition rate is weighted by appropriate thermal factor. This model therefore includes all the processes discussed in Sec. II. This model is valid only at low temperatures where the contributions from the LH excitons and free carriers is negligible. This is a good assumption in our case because the LH emission was more than one order-of-magnitude weaker than the HH emission in the worst case (the highest T investigated).

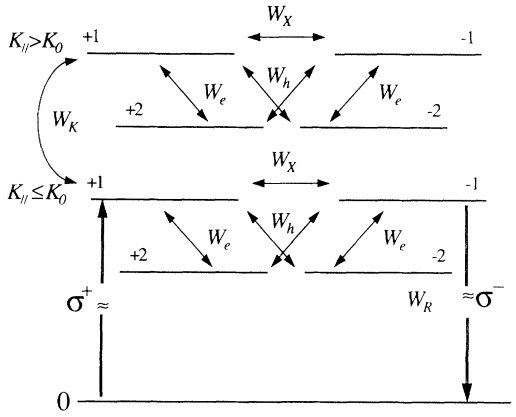

FIG. 2. Model for the exciton dynamics as discussed in the text.

Considering a Gaussian excitation pulse generation rate $G(t)$, the evolution of the population in each state is given by a set of eight coupled equations:

$$\frac{d}{dt}N_i=F_{ij}N_j+G(t)\delta_{+1,i}\ , \tag{6}$$

where N_i is the column vector (N_{+1} N_{-1} N_{+2} $N_{-2}N_{+1k}$ N_{-1k} N_{+2k} N_{-2k}) and F is a 8×8 matrix:

$$F=\begin{bmatrix} A & B & C & 0 \\ D & E & 0 & C \\ F & 0 & G & B \\ 0 & F & D & H \end{bmatrix}\ ,$$

where A through H are the following 2×2 matrices:

$$A=\begin{bmatrix} -(W_R+W_X+W_{em}+W_{hm}+W_{kp}) & W_X \\ W_X & -(W_R+W_X+W_{em}+W_{hm}+W_{kp}) \end{bmatrix},$$

$$B=\begin{bmatrix} W_{ep} & W_{hp} \\ W_{hp} & W_{ep} \end{bmatrix},\quad C=\begin{bmatrix} W_{km} & 0 \\ 0 & W_{km} \end{bmatrix},\quad D=\begin{bmatrix} W_{em} & W_{hm} \\ W_{hm} & W_{em} \end{bmatrix},$$

$$E=\begin{bmatrix} -(W_{ep}+W_{hp}+W_{kp}) & 0 \\ 0 & -(W_{ep}+W_{hp}+W_{kp}) \end{bmatrix},\quad F=\begin{bmatrix} W_{kp} & 0 \\ 0 & W_{kp} \end{bmatrix},$$

$$G=\begin{bmatrix} -(W_{km}+W_X+W_{em}+W_{hm}) & W_X \\ W_X & -(W_{km}+W_X+W_{em}+W_{hm}) \end{bmatrix},$$

$$H=\begin{bmatrix} -(W_{km}+W_{ep}+W_{hp}) & 0 \\ 0 & -(W_{km}+W_{ep}+W_{hp}) \end{bmatrix},$$

and 0 is a 2×2 null matrix. W_R and W_X are the radiative and exciton spin-relaxation rate, respectively. W_{ep} and W_{em} are the electron spin-relaxation rates within an exciton with proper consideration for the occupation of states and are given by the following expressions:

$$W_{ep}=W_e\left[\frac{1}{\left[1+\exp\left[\frac{\Delta}{k_BT}\right]\right]}\right],$$

$$W_{em}=W_e\left[\frac{1}{\left[1+\exp\left[-\frac{\Delta}{k_BT}\right]\right]}\right],$$

where Δ is the exchange splitting, commonly assumed of the order of 0.1 meV,[37] W_e is the electron spin-relaxation rate, and T is the lattice temperature. Similar relations hold for the hole-spin relaxation rates $W_{hp(m)}$. Similarly, the acoustic-phonon scattering rates $W_{kp(m)}$ are defined as

$$W_{kp}=W_k\exp\left[-\frac{\Gamma_h}{k_BT}\right],$$

$$W_{km}=W_k\left[1-\exp\left[-\frac{\Gamma_h}{k_BT}\right]\right],$$

where W_k is the effective scattering rate with phonons.

Although there are six parameters in the model, we now show that reliable quantitative information about these rates can be obtained by fitting the experimental results with this model. This is because Γ_h is independently determined, W_R can be determined from W_D, and different parameters affect different combinations of the measured polarized luminescence dynamics.

We begin the fit by determining W_R from W_D, the long-time decay constant of S, using the value of Γ_h determined independently from the FWM measurements. The sum S is independent of W_X because W_X does not change the total population of excitons in the two radiative states. Numerical simulations show that S is sensitive to W_k and Γ_h, but not to W_h and W_e. In Fig. 3, we therefore keep W_e and W_h constant and explore the effects of changing Γ_h and W_k. Figure 3(a) shows the effects of changing Γ_h by 50% and keeping W_k constant. Increasing Γ_h reduces W_R (since W_D is fixed) and hence makes the initial drop of S slower, and makes the fit noticeably worse. The fit quality can be improved by a

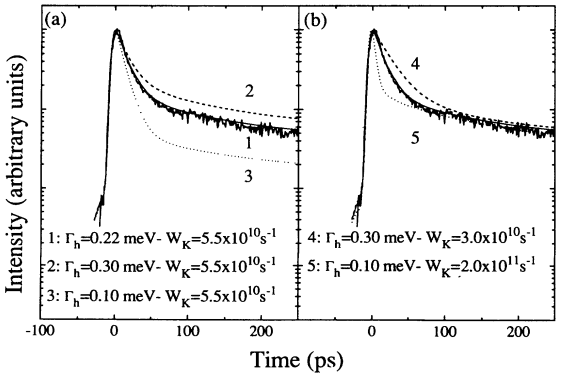

FIG. 3. Comparison of different fits to the sum S for the 150-Å QW at 12 K as discussed in the text.

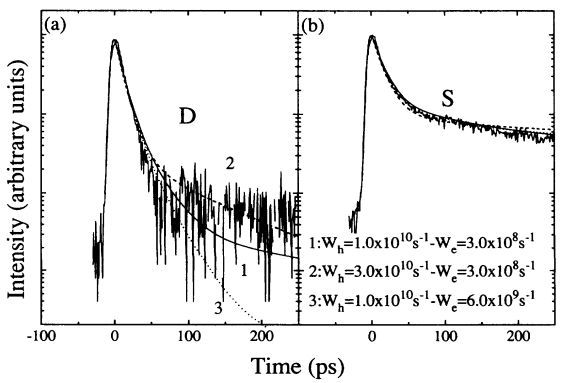

FIG. 4. Comparison of different fits to the difference D and the sum S for the 150-Å QW at 12 K as discussed in the text.

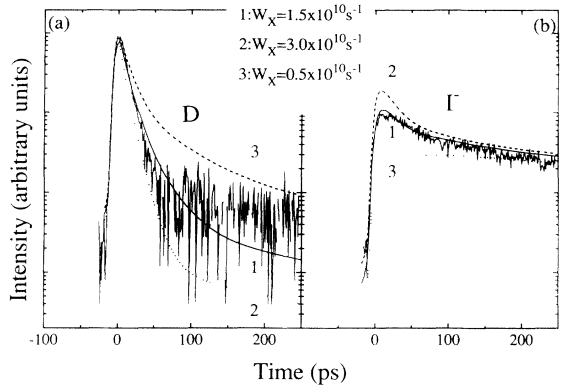

FIG. 5. Comparison of different fits to the difference D and I^- for the 150-Å QW at 12 K as discussed in the text.

change of W_k [Fig. 3(b)] but the initial dynamics can still not be reproduced satisfactorily. Extensive analysis shows that acceptable fits can only be obtained for a certain range of each parameter.

Figure 4 shows that a change in W_h and W_e affects S weakly, but strongly modifies the decay of the difference D at longer time. A change in W_X strongly affects both I^- and D (Fig. 5). Figures 3–5 therefore demonstrate that, despite the large number of parameters, reliable values for them can be extracted from a careful fit procedure of the four experimental curves. The best fits obtained by this procedure for the data of Fig. 1 are shown in the figure.

VI. ANALYSIS AND DISCUSSION OF RESULTS

A. 150-Å quantum well at 12 K

The results for the 150-Å quantum-well sample at 12 K and without any applied bias were discussed in detail earlier.[23] We discuss here some important aspects of those results.

The best fits to the data for this sample are also shown in Fig. 1. As discussed above, $W_D = 1.54\times10^9\ s^{-1}$ is obtained directly by fitting the long-time slope of the total PL intensity (S). From this we deduce a value of $W_R = 1.7\times10^{10}\ s^{-1}$, corresponding to a radiative decay time of about 60 ps. As discussed above and also earlier,[23] W_e and W_h do not affect the fits to S significantly so W_k and W_h are the primary parameters for obtaining fits to S. We find that the best fits are obtained by $\Gamma_h = 0.22\pm0.02$ meV (in good agreement with the results of FWM measurements) and $W_k = (5.5\pm1.5)\times10^{10}\ s^{-1}$. The error bars are obtained by the procedure discussed above in Sec. V. From these fits, we deduce that approximately 50% of the initial decay of the PL intensity can be attributed to the radiative decay of the resonantly-excited excitons, and the remaining 50% to the scattering out of the small K to the large K states by acoustic phonons. We conclude from this analysis that (1) the radiative decay rate of the 2D exciton polaritons is indeed enhanced as predicted theoretically, (2) the initial decay of the PL cannot be simply regarded as due to either of these processes individually. The latter reaffirms our statements that a comprehensive analysis considering all the scattering processes is essential for a correct understanding of the dynamics of excitons.

The temporal evolution of I^- is determined primarily by the spin-flip rate of excitons and the best fit to the data yields $W_X = (1.5\pm0.5)\times10^{10}\ s^{-1}$. The behavior of D beyond 50 ps is quite sensitive to W_h and best fits yield W_h between 0.7 and $1\times10^{10}\ s^{-1}$. Under our assumption that $W_e < W_h$, the fits are not sensitive to W_e and we can only put lower and upper bounds on the values of W_e: $3\times10^8 < W_e < 3\times10^9\ s^{-1}$.

From the value of W_R deduced above, we find [Eq. (3)] that $2\Gamma_0 = 2.5\times10^{10}\ s^{-1}$, corresponding to a radiative recombination time of 40 ps. This time is a factor of 2 larger than that calculated theoretically.[20] The reason for this discrepancy is not clear at this time, but there are a few possibilities that must be considered. First of all, the value of E_0 depends on the in-plane mass of the exciton and there may be an uncertainty of 30–40 % in its value. Also, as discussed in the previous section, we are deducing an average value of $2\Gamma_0$ from $K_\parallel = 0$ and K_0, while the theoretical value is for $K_\parallel = 0$. The role of other collisions with surface imperfections or phonons, which, reducing the exciton coherence area, can lead to longer decay times,[36] must also be considered. Further investigations will be necessary to understand this question.

B. Well-width dependence

The results for the three different samples we investigated do not show any striking differences as shown in Fig. 6 where the decays are compared for the 80- and 150-Å QW's at 12 K. With decreasing well width, we observe a faster rise of I^- and a steeper slope of S at long times. The latter finding shows that W_D increases as the well thickness is reduced, in agreement with previous results from nonresonant experiments.[11]

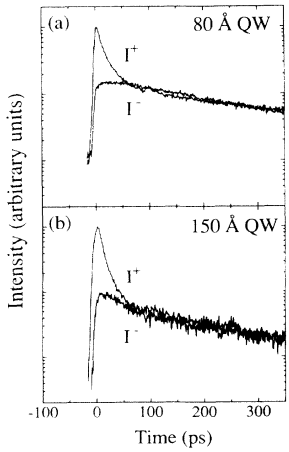

FIG. 6. Comparison of the PL decay for two samples at 12 K at low excitation intensity. (a) Time evolution of I^+ and I^- for the 80-Å QW. (b) Time evolution of I^+ and I^- for the 150-Å QW.

Although there are no dramatic changes observed in the measured luminescence profiles, best fits to the model for the four temporal evolutions of each sample allow us to determine the values of various scattering rates for the different samples. In Fig. 7 the most important rates obtained from the fits at 12 K are compared for the different samples. We show the dependence of $2\Gamma_0$, W_X, and W_k as a function of the well width. We find that $2\Gamma_0$ increases as the well width is reduced. This occurs because of increased overlap of the electron and hole wave functions and is in agreement with the theoretical dependence of the oscillator strength.[34] W_k increases as $1/L$ as expected [Eq. (2)] for the interaction of exciton with phonons through deformation potential.[28] W_X also increases with a reduction in the well width. This is because a reduction in the well width leads to an increased overlap of the electron-hole wave functions which enhances the exchange interaction responsible for the spin flip of excitons.[21] A more controlled way of varying this overlap by applying an electric field along the growth direction will be discussed in Sec. VI D.

C. Temperature and intensity dependence

In Fig. 8 the PL decays at two different temperatures are compared for the 130-Å QW. The major difference is that the initial drop in PL intensity becomes more important with increasing T both for I^+ and I^-; this feature is more pronounced for the 130- and 80-Å QW's, while there is not much change in the initial PL decay for the 150-Å QW between 12 and 27 K. We chose to limit ourselves to a small temperature range because light-hole and free-carrier recombination becomes important at higher temperature,[38] making the analysis of the exciton dynamics more complicated. With increasing temperature, the exponential decay of S at long delays becomes slower, in agreement with previous results.[11] This finding and the fact that the PL quantum yield is constant in the explored temperature range show that the nonradiative processes are negligible in our samples.

Contrary to previous results[15] our data clearly show that the fast drop of I^+ persists at higher T at least up to 40 K. Since Γ_h increases significantly with temperature, this relative insensitivity of the initial decay to temperature is a further evidence that the initial dynamics is not due to a loss of interband coherence.

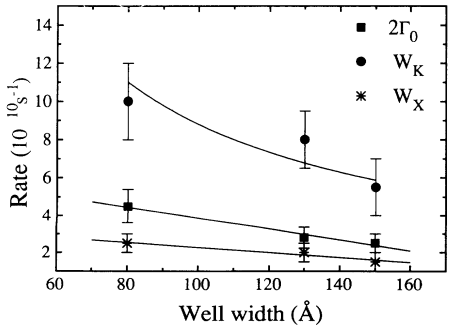

FIG. 7. Different rates as obtained from fits to the experimental data at 12 K and low excitation intensity for 80-, 130-, and 150-Å QW's. The solid lines are guides for eyes.

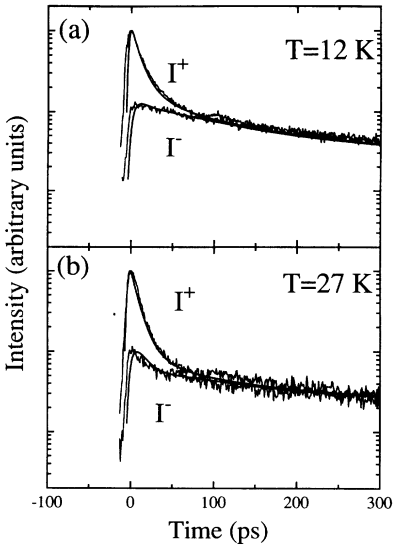

FIG. 8. Comparison of the PL decay at two different temperatures for the 130-Å QW. (a) I^+ and I^- at 12 K. (b) I^+ and I^- at 27 K. Also shown are the fits to the experimental data.

The main effect of raising the temperature is to increase both Γ_h and W_k. From the fit we deduce that Γ_h increases linearly with a slope that for the 150-Å QW is 5 μeV/K, in agreement with earlier results.[24] Besides the product $\Gamma_h \times W_R$ remains constant for all the samples as expected from Ref. 36. W_k increases with temperature for the 150-Å QW, while it remains fairly constant for the 80- and 130-Å QW's; in any case, the rate of increase is slower than expected. This is partly because of the increase of Γ_h with temperature which makes it more difficult to scatter out of the small K region (W_k is an effective scattering rate) and partly because of our simplified model which reduces the manifold of K states two sets of states.

W_X decreases slightly with temperature. This dependence is expected if we consider a motional-narrowing mechanism for the spin relaxation with W_X proportional to the momentum relaxation time τ^*; if we assume τ^* equal to the dephasing time T_2, an increase of T decreases T_2 and leads to a decreased exciton spin-relaxation rate. No dependence is found for W_h and W_e, either on the quantum-well width or on the temperature: as previously observed, the fits, with no field applied, are not very sensitive to these two parameters.

In Fig. 9 the PL decays are compared for two different excitation intensities for the 150-Å QW. Again some changes occur in the first hundreds of picoseconds but, contrary to previous reports,[15] the overall PL temporal profile remains substantially unmodified, except that a long-time component appears in the decay of D. This slow component is found also when an electric field is applied and its origin will be discussed in the following section. No systematic quantitative analysis has been performed for the intensity-dependent data, in view of the fact that other processes, in particular exciton-exciton interaction, can play an important role (note the poorer

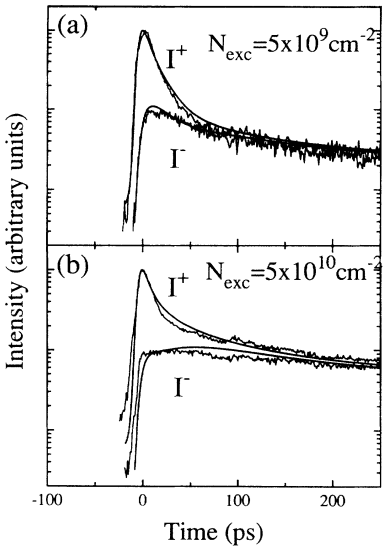

FIG. 9. Comparison of the PL decay at two different excitation intensities for the 150-Å QW. (a) I^+ and I^- at $N_{exc}=5\times10^9$ cm^{-2}. (b) I^+ and I^- at $N_{exc}=5\times10^{10}$ cm^{-2}. Also shown are the fits to the experimental data.

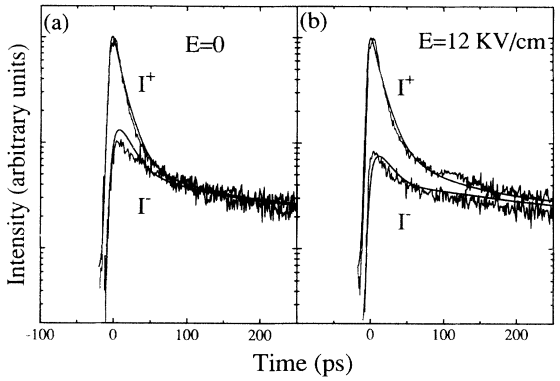

FIG. 10. PL decay of the 150-Å QW at 20 K for two different electric fields E, along the growth direction. (a) $E=0$. (b) $E=12$ KV/cm. Also shown are the fits to the experimental data.

quality of the fit with respect to the low-intensity results). The qualitative general trend of increasing Γ_h and W_k with increasing intensity is consistent with increased dephasing rate and more important contribution of scattering events which scatter excitons out of the homogeneously broadened radiative region at high density. We note that the temperature range was such that, even at the highest excitation intensity, Γ_h was always smaller than k_BT. Therefore no information can be extracted about the exciton-exciton interaction as a mechanism producing an increase of the exciton lifetime, because the dependence of W_D on Γ_h is cancelled in Eqs. (3) and (5).[17] By a comparison with the results of Ref. 17 it turns out that we are focusing on different aspects; in the case of Ref. 17, Γ_h was greater than k_BT, allowing Eccleston *et al.* to evidence the dependence of W_D on the dephasing time when the excitation intensity was increased, but they attributed to RRS and surface scattered laser light the initial PL signal, while our improved time resolution allows us to prove that important physical information can be extracted from the initial PL decay.

D. Electric-field dependence

As is well known, an electric field along the growth direction leads to a change in the overlap between the electron and hole wave functions. One effect of this change is to reduce the radiative transition probability which has been explored before.[39] The other effect is to change the exchange interaction responsible for the exciton spin flip. The latter has not been explored previously except for our recent report,[40] and is the main motivation behind our experiments with applied electric field. We note that W_R depends on the square of the overlap integral,[41] while W_X depends on the fourth power of the overlap integral. Therefore, the decrease of W_X in the presence of a field should be the dominant effect at least at low fields.

In Fig. 10, we show the PL temporal profiles for two different longitudinal electric fields E applied to the quantum-well structure along the growth direction. As shown for the 150-Å QW, under the flat band condition I^+ and I^- equilibrate in $\sim$100 ps. Applying a field of 12 KV/cm it takes roughly twice the time for reaching the same condition. As a consequence (Fig. 11), at zero field the difference decays to the noise level quite fast (with a time constant of 12 ps). At higher fields, the initial fast decay is still present but a longer tail (300 ps) appears which becomes more important at higher field. We want to emphasize that the long tail is very similar to the one found in the high-intensity data, suggesting the same physical origin. No change in the sum S is observed for the various fields.

As discussed in Sec. II, the spin relaxation of the exciton can proceed in two different ways (one-step process with rate W_X and two-step process with rates W_e and W_h). A reduction in W_X would make the contribution of the two-step process more important. The long tail in the decay of D can therefore be correlated with the increasing importance of the electron and hole spin flips relative to the exciton spin flip. The fact that the slow slope of D

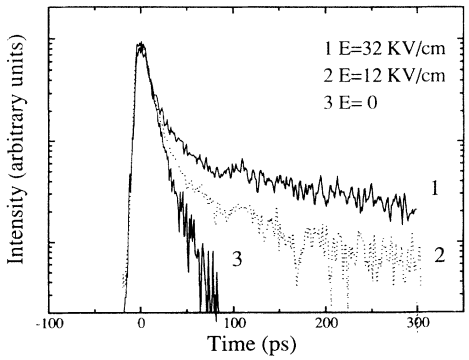

FIG. 11. PL decay of the difference D for three different electric fields E for the 150-Å QW at 20 K.

is independent of the electric field proves that W_e and W_h are not affected by the field, at least in this range of field. The slow tail should, in principle, be present also at low fields but is too weak to be detected in our data, at least at the lowest excitation intensity. The independence of S on the electric field is a further evidence that the change of D with field is due to a change of W_X, because S is independent of W_X but depends on all the other rates. We do not find measurable change for W_R with electric field in the investigated range within the experimental error, due to the limited delay range (up to 1.5 ns); the value of W_X is not sensitive to W_R in this field range and therefore reliable values can be obtained by this procedure.

From best fits to the data at various electric fields, we determine the values of W_X, W_e, and W_h. The dependence of W_X on electric field was recently calculated by a variational calculation.[21,40] In Fig. 12(a) the W_X determined from our experimental results is compared with the theoretical calculation for 185-Å and 160-Å QW's with infinite barriers. The 185-Å QW with infinite barriers produces the same confinement energy as the 150-Å QW with barrier of $Al_{0.3}Ga_{0.7}As$. The experimental trend is very similar to the theoretical one, and there is a reasonably good agreement between the theory and the experiment. The stronger theoretical dependence on the field may be due to some approximations in the description of the exciton wave function which overestimate the change of the overlap integral with the field. Concerning the absolute values of W_X in comparison with the theoretical ones assuming a motional-narrowing mechanism, we find a discrepancy of about a factor 2.5. As discussed in more details in Ref. 40, this can be attributed to

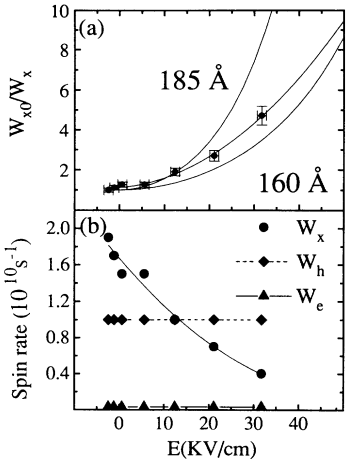

FIG. 12. (a) Dependence of the spin-relaxation rate W_X for the 150-Å QW as deduced from fits to the experimental data, as a function of the applied field. The continuous line connecting the experimental point is a quadratic fit. W_{X0} is the value at flat band. Also shown is the theoretically calculated dependence for the same quantity for two wells of 160 and 185 Å thicknesses and infinite barriers. (b) Dependence of the various spin-relaxation rates W_X, W_h, and W_e on the applied field for the 150-Å QW as deduced from fits to the experimental data at 20 K. The lines connecting the experimentally deduced values are only guides for eyes.

an approximate description of the center-of-mass motion in the theoretical model for the exciton spin relaxation and to the assumption of the momentum relaxation time τ^* equal to T_2.

In Fig. 12(b) the different spin relaxation rates for the exciton, electron, and hole are compared as a function of the field. While no dependence is found for W_e and W_h in the explored range, W_X decreases by roughly a factor 5 so that W_h become larger than W_X above a certain electric field. This leads to the increased importance of the dark states and hence the slow tail in D. However, W_e is so small that the transitions between the $|+1\rangle$ and the $|-1\rangle$ exciton states continue to be dominated by W_X, i.e., mainly driven by the exchange interaction. We want to emphasize that our data as a function of the field represent the first clear measurement of the contribution of the dark states of the excitons and show that, even in wide wells, the exchange interaction is the dominant mechanism for relaxing the spin of the exciton between optically-allowed exciton states.

VII. CONCLUSIONS

We have shown that several different processes, occurring on the same time scale, control the initial dynamics of cold nonequilibrium excitons and determine the dynamics from the nonthermal to the thermal regime. These processes include the enhanced radiative recombination of the metastable 2D exciton polariton, the spin relaxation of excitons between the $|\pm1\rangle$ optically-allowed exciton states, the spin relaxation of electron or hole coupling the optically-allowed $|\pm1\rangle$ exciton states with the dark exciton states $|\pm2\rangle$, and the scattering of excitons between different exciton momentum (wave vector) states for the center-of-mass motion of excitons. We have also shown that a simultaneous investigation of these processes and a unified analysis of the results, as presented here, are essential for a proper understanding of the initial exciton dynamics and for extracting quantitative information about the radiative, spin-relaxation, and momentum-relaxation rates of excitons.

By measuring time-resolved luminescence intensity profiles of various polarization components following resonant excitation and analyzing the results with a unified model, we have extracted quantitative values for these rates as a function of quantum-well width, temperature, excitation intensity, and applied electric field. Several conclusions can be drawn from this investigation: (1) The enhanced radiative recombination of 2D exciton-polariton contributes about 50% to the initial decay of the luminescence intensity of resonantly-excited excitons under the conditions of our experiments. The value of the intrinsic radiative rate determined from our investigations is about $\frac{1}{40}$ ps for the 150-Å QW, approximately a factor of 2 slower than theoretically predicted. (2) The second leading cause of the initial decay of the resonantly-excited exciton luminescence is the scattering of excitons to nonradiative large K excitons by acoustic phonons. This rate varies inversely with the quantum-well width and is expected to be a strong function of temperature. (3) It takes more than a hundred picoseconds

for the resonantly-excited excitons to thermalize for the conditions of our experiment. These times are not too different from the thermalization times of nonresonantly created excitons determined in our earlier studies. (4) One of the crucial points that comes out from our work opposite to previous conclusions by other authors is that the temporal profile of resonantly-excited excitonic luminescence is neither simply a manifestation of loss of interband coherence nor simply an evidence of fast excitonic recombination. (5) An important contribution of our work concerns the spin relaxation of excitons. We have shown that the exchange interaction is the dominant mechanism for relaxing the spin between the optically-allowed exciton states even in wide wells. We have also shown that a suitable way of varying the contribution of exchange- and single-particle spin flips is to apply an electric field or change the well width. We have determined both contributions and found a reasonably good agreement with a theoretical model for the exciton spin relaxation.

There are still some open questions and problems. We would like to mention the investigation of the role of light-hole exciton and eventually free carriers at high temperature in the recombination process. Also, the discrepancy of about a factor of 2 between the theoretical and experimentally determined values of the radiative recombination and exciton spin-flip relaxation rate needs further attention. A more refined model of scattering of excitons between different momentum states of excitons would also be important. Investigations on these topics are under progress.

ACKNOWLEDGMENTS

A.V. thanks AT&T Bell Laboratories in Holmdel (NJ), for offering the possibility of performing this research. We also acknowledge K. W. Goossen for help in processing the sample. M.Z.M. and L.J.S. are partially supported by NSF Grant No. DMR 91-17298.

*Permanent address: Dipartimento di Fisica dell'Università, Largo E. Fermi 2, 501 25 Firenze, Italy.

[1]See, for instance, E. O. Göbel, in *Excitons in Confined Systems*, edited by R. Del Sole, A. d'Andrea, and A. Lapiccirella, Springer Proceeding in Physics Vol. 25 (Springer-Verlag, Berlin, 1988), p. 204; Proceedings of Third International Conference on Optics of Excitons in Confined Systems, Montpellier, 1993 [J. Phys. (Paris) Colloq. **3**, C5 (1993)].

[2]See, for instance, S. Schmitt-Rink, D. S. Chemla, and D. A. B. Miller, Phys. Rev. B **32**, 6601 (1985); J. P. Sokoloff, M. Joffre, B. Fuegel, D. Hulin, M. Lindberg, S. W. Koch, A. Migus, A. Antonetti, and N. Peyghambarian, *ibid.* **38**, 7615 (1988).

[3]T. C. Damen, Jagdeep Shah, D. Y. Oberli, D. S. Chemla, J. E. Cunningham, and J. M. Kuo, Phys. Rev. B **42**, 7434 (1990).

[4]J. Kusano, Y. Segawa, T. Aoyagi, S. Namba, and H. Okamoto, Phys. Rev. B **40**, 1685 (1989).

[5]R. Eccleston, R. Strobel, W. W. Rühle, J. Kuhl, B. F. Feuerbacher, and K. Ploog, Phys. Rev. B **44**, 1395 (1991).

[6]Ph. Roussignol, C. Delalande, A. Vinattieri, L. Carraresi, and M. Colocci, Phys. Rev. B **45**, 6965 (1992).

[7]J. P. Bergman, P. O. Holtz, B. Monemar, M. Sundaram, J. L. Merz, and A. C. Gossard, Phys. Rev. B **43**, 4765 (1991).

[8]T. C. Damen, Karl Leo, Jagdeep Shah, and J. E. Cunningham, Appl. Phys. Lett. **58**, 1902 (1991).

[9]H. Chao, K. S. Wong, R. R. Alfano, H. Unlu, and H. Morkoc, Ultrafast Laser Probe Phenomena in Bulk and Microstructure Semiconductors II [Proc. SPIE **942**, 215 (1988)]; J. Snelling, A. S. Plaut, G. P. Flinn, A. C. Tropper, R. T. Harley, and T. M. Kerr, J. Lumin. **45**, 208 (1990); Ph. Roussignol, P. Rolland, R. Ferreira, C. Delalande, G. Bastard, A. Vinattieri, L. Carraresi, M. Colocci, and B. Etienne, Surf. Sci. **267**, 360 (1992); B. Dareys, X. Marie, T. Amand, J. Barrau, Y. Shekun, I. Razdobreev, and R. Planel, Superlatt. Microstruct. **13**, 353 (1993); V. Srinivas, Y. J. Chen, and C. E. C. Wood, Phys. Rev. B **47**, 10 907 (1993); A. Frommer, E. Cohen, A. Ron, and L. N. Pfeiffer, *ibid.* **48**, 2803 (1993).

[10]T. C. Damen, L. Viña, J. E. Cunningham, Jagdeep Shah, and L. J. Sham, Phys. Rev. Lett. **67**, 3432 (1991); Ph. Roussignol, P. Rolland, R. Ferriera, C. Delalande, G. Bastard, A. Vinattieri, J. Martinez-Pastor, L. Carraresi, M. Colocci, J. F. Palmier, and B. Etienne, Phys. Rev. B **46**, 7292 (1992); J. Wagner, H. Schneider, D. Richards, A. Fischer, and K. Ploog, *ibid.* **47**, 4786 (1993).

[11]J. Feldmann, G. Peter, E. O. Göbel, P. Dawson, K. Moore, G. Foxon, and R. J. Elliot, Phys. Rev. Lett. **59**, 2337 (1987); M. Gurioli, A. Vinattieri, M. Colocci, C. Deparis, J. Massies, G. Neu, A. Bosacchi, and S. Franchi, Phys. Rev. B **44**, 3115 (1991); V. Srinivas, J. Hryniewicz, Y. J. Chen, and E. C. Wood, *ibid.* **46**, 10 193 (1992); J. Martinez-Pastor, A. Vinattieri, L. Carraresi, M. Colocci, Ph. Roussignol, and G. Weimann, *ibid.* **47**, 10 456 (1993).

[12]G. W. 't Hooft, W. A. J. A. van der Poel, L. W. Molenkamp, and C. T. Foxon, Phys. Rev. B **35**, 8281 (1987).

[13]W. H. Knox, R. L. Fork, M. C. Downer, D. A. B. Miller, D. S. Chemla, C. V. Shank, A. C. Gossard, and W. Wiegmann, Phys. Rev. Lett. **54**, 1306 (1985).

[14]S. Bar-Ad and I. Bar-Joseph, Phys. Rev. Lett. **68**, 349 (1992); J. B. Stark, W. H. Knox, and D. S. Chemla, Phys. Rev. B **46**, 7919 (1992).

[15]B. Deveaud, F. Clérot, N. Roy, K. Satzke, B. Sermage, and D. S. Katzer, Phys. Rev. Lett. **67**, 2355 (1991).

[16]B. Sermage, B. Deveaud, K. Satzke, F. Clérot, C. Dumas, N. Roy, D. S. Katzer, F. Mollot, R. Planel, M. Berz, and J. L. Oudar, Superlatt. Microstruct. **13**, 271 (1993); B. Sermage, S. Long, B. Deveaud, and D. S. Katzer, J. Phys. IV (Paris) Colloq. **3**, C5-19 (1993).

[17]R. Eccleston, B. F. Feuerbacher, J. Kuhl, W. W. Rühle, and K. Ploog, Phys. Rev. B **45**, 11 403 (1992).

[18]J. J. Hopfield, Phys. Rev. **112**, 1555 (1958).

[19]E. Hanamura, Phys. Rev. B **38**, 1228 (1988).

[20]L. C. Andreani, F. Tassone, and F. Bassani, Solid State Commun. **77**, 641 (1991); F. Tassone, F. Bassani, and L. C. Andreani, Nuovo Cimento **12**, 1673 (1990); L. C. Andreani, in *Confined Electrons and Photons: New Physics and Devices*, edited by E. Burstein and C. Weisbuch (Plenum, New York, in press).

[21]M. Z. Maialle, E. A. de Andrada e Silva, and L. J. Sham, Phys. Rev. B **47**, 15 776 (1993); M. Z. Maialle and L. J. Sham, Proceedings of the 10th International Conference on Electronic Properties of Two-dimensional Systems, Newport,

1993 [Surf. Sci. (to be published)].

[22]T. Uenoyama and L. J. Sham, Phys. Rev. Lett. **64**, 3070 (1990); R. Ferreira and G. Bastard, Phys. Rev. B **43**, 9687 (1991).

[23]A. Vinattieri, Jagdeep Shah, T. C. Damen, D. S. Kim, L. N. Pfeiffer, and L. J. Sham, Solid State Commun. **88**, 189 (1993); A. Vinattieri, Jagdeep Shah, T. C. Damen, D. S. Kim, L. N. Peiffer, and L. J. Sham, J. Phys. IV (Paris) Colloq. **3**, C5-27 (1993); A. Vinattieri, Jagdeep Shah, T. C. Damen, L. N. Pfeiffer, L. J. Sham, and M. Z. Maialle, in *Ultrafast Phenomena in Semiconductors,* edited by David K. Ferry and Henry M. van Driel [Proc. SPIE **2142**, 2 (1994)].

[24]L. Schultheis, A. Honold, J. Kuhl, K. Köhler, and C. W. Tu, Phys. Rev. B **34**, 9027 (1986).

[25]J. Hegarty, M. D. Sturge, C. Weisbuch, A. C. Gossard, and W. Wiegmann, Phys. Rev. Lett. **49**, 930 (1982).

[26]H. Stolz, D. Schwarze, W. von der Osten, and G. Weimann, Phys. Rev. B **47**, 9669 (1993); H. Stolz, in *Ultrafast Phenomena in Semiconductors,* edited by David K. Ferry and Henry M. van Driel [Proc. SPIE **2142**, 170 (1994)].

[27]See, for instance, S. T. Cundiff and D. G. Steel, IEEE J. Quantum Electron. **QE-28**, 2423 (1992); Proceedings of the Third International Workshop on Nonlinear Optics and Excitation Kinetics in Semiconductors, Bad Honnef, 1992 [Phys. Status Solidi B **173**, (1992)].

[28]Johnson Lee, E. S. Koteles, and M. O. Vassel, Phys. Rev. B **33**, 5512 (1985).

[29]P. K. Basu and Parta Ray, Phys. Rev. B **45**, 1907 (1992).

[30]M. I. D'yakonov and V. I. Perel, Zh. Eksp. Teor. Fiz. **60**, 1954 (1971) [Sov. Phys. JETP **33**, 1053 (1971)].

[31]L. C. Andreani and F. Bassani, Phys. Rev. B **41**, 7536 (1990).

[32]W. J. Rappel, L. F. Feiner, and M. F. H. Schuurmans, Phys. Rev. B **38**, 7874 (1988).

[33]V. M. Agranovich, in *Optics of Excitons in Confined Systems,* edited by A. D'Andrea, R. Del Sole, R. Girlanda, and A. Quattropani, IOP Conf. Proc. No. 123 (Institute of Physics and Physical Society, London, 1992), p. 1; V. M. Agranovich and O. A. Dubovsky, Pis'ma Zh. Eksp. Teor. Fiz. **3**, 345 (1966) [JETP Lett. **3**, 223 (1966)]; V. M. Agranovich and S. Mukamel, Phys. Lett. A **147**, 155 (1990).

[34]L. C. Andreani and A. Pasquarello, Phys. Rev. B **42**, 8928 (1990).

[35]Jagdeep Shah, IEEE J. Quantum Electron. **QE-24**, 276 (1988).

[36]D. S. Citrin, Solid State Commun. **84**, 281 (1992); Phys. Rev. B **47**, 3832 (1993).

[37]W. Ekardt, K. Lösch, and D. Bimberg, Phys. Rev. B **20**, 3303 (1979).

[38]M. Colocci, M. Gurioli, and A. Vinattieri, Phys. Scr. **T39**, 211 (1991).

[39]H. P. Polland, L. Schultheis, J. Kuhl, E. O. Göbel, and C. W. Tu, Phys. Rev. Lett. **55**, 2610 (1985).

[40]A. Vinattieri, Jagdeep Shah, T. C. Damen, K. W. Goossen, L. N. Pfeiffer, M. Z. Maialle, and L. J. Sham, Appl. Phys. Lett. **63**, 3164 (1993).

[41]G. Bastard, E. E. Mendez, L. L. Chang, and L. Esaki, Phys. Rev. B **28**, 3241 (1983).